

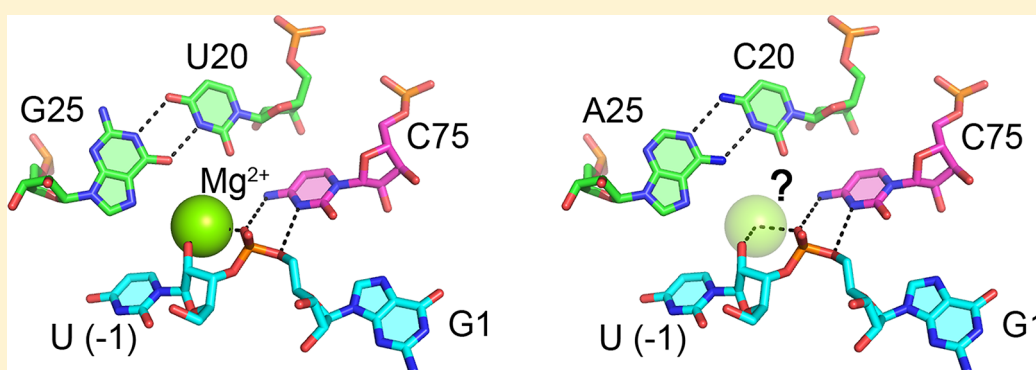
Identification of the Catalytic Mg^{2+} Ion in the Hepatitis Delta Virus Ribozyme

Ji Chen,[†] Abir Ganguly,^{‡,||} Zulaika Miswan,[†] Sharon Hammes-Schiffer,^{‡,||} Philip C. Bevilacqua,^{*,‡,§} and Barbara L. Golden^{*,†}

[†]Department of Biochemistry, Purdue University, 175 South University Street, West Lafayette, Indiana 47907, United States

[‡]Department of Chemistry and [§]Center for RNA Molecular Biology, The Pennsylvania State University, University Park, Pennsylvania 16802, United States

S Supporting Information



ABSTRACT: The hepatitis delta virus ribozyme catalyzes an RNA cleavage reaction using a catalytic nucleobase and a divalent metal ion. The catalytic base, C75, serves as a general acid and has a pK_a shifted toward neutrality. Less is known about the role of metal ions in the mechanism. A recent crystal structure of the precleavage ribozyme identified a Mg^{2+} ion that interacts through its partial hydration sphere with the G25·U20 reverse wobble. In addition, this Mg^{2+} ion is in position to directly coordinate the nucleophile, the 2'-hydroxyl of U(−1), suggesting it can serve as a Lewis acid to facilitate deprotonation of the 2'-hydroxyl. To test the role of the active site Mg^{2+} ion, we replaced the G25·U20 reverse wobble with an isosteric A25·C20 reverse wobble. This change was found to significantly reduce the negative potential at the active site, as supported by electrostatics calculations, suggesting that active site Mg^{2+} binding could be adversely affected by the mutation. The kinetic analysis and molecular dynamics of the A25·C20 double mutant suggest that this variant stably folds into an active structure. However, pH-rate profiles of the double mutant in the presence of Mg^{2+} are inverted relative to the profiles for the wild-type ribozyme, suggesting that the A25·C20 double mutant has lost the active site metal ion. Overall, these studies support a model in which the partially hydrated Mg^{2+} positioned at the G25·U20 reverse wobble is catalytic and could serve as a Lewis acid, a Brønsted base, or both to facilitate deprotonation of the nucleophile.

The hepatitis delta virus (HDV) ribozymes were originally identified in the genomic and antigenomic RNAs produced by the human hepatitis delta virus and are integral to the viral life cycle. These ribozymes have a conserved secondary structure comprised of five short base-paired double helices arranged in a double-pseudoknotted topology (Figure 1).^{1,2} Key nucleotides in the active site are conserved (Figure 1). For many years, these ribozymes were believed to be rare in nature and found only within HDV RNAs. Recently, however, HDV-like ribozymes have been discovered in a wide variety of organisms, where they may play essential roles in the regulation of gene expression.^{3–7}

Similar to other small nucleolytic ribozymes, the HDV ribozyme activates the 2'-hydroxyl of the nucleotide upstream of the scissile phosphate for nucleophilic attack at the scissile phosphate. This reaction results in the formation of products

that contain 2',3'-cyclic phosphate and 5'-hydroxyl termini. Many of the small nucleolytic ribozymes use nucleobases in their catalytic mechanisms.⁸ These nucleobases often appear to serve as general acids, donating a proton to the 5'-hydroxyl leaving group. Both the HDV ribozyme and the hairpin ribozyme shift the pK_a of the general acid (C75 for the HDV ribozyme and A38 for the hairpin ribozyme) toward neutrality, thereby increasing reactivity.^{9,10} In addition, hammerhead, hairpin, and VS ribozymes have guanosine bases in good position to serve as a general base,^{11–13} although other roles such as positioning and electrostatic stabilization remain

Received: September 26, 2012

Revised: December 21, 2012

Published: January 11, 2013



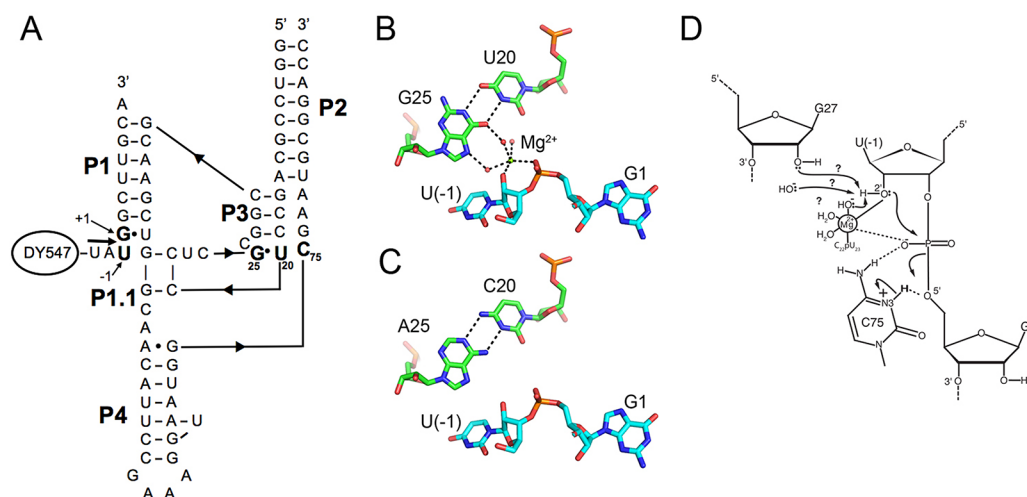


Figure 1. Structure of the HDV ribozyme. (A) Secondary structure of the two-piece WT HDV ribozyme used in this study, showing the substrate strand with its attached fluorophore, DY547. Nucleotides U(−1), G1, G25, U20, and C75 are shown in bold and numbered. This is the same RNA used in our precleavage crystal structure.²⁹ The numbering starts again in the truncated P4 to be consistent with the WT ribozyme. (B) Tertiary structural features of the WT ribozyme from Protein Data Bank entry 3NKB²⁹ showing the G25·U20 reverse wobble, the cleavage site dinucleotide, and the active site Mg²⁺ ion. (C) Isosteric reverse wobble that could form in the A25·C20 double mutant. Note that the Mg²⁺ ion is present in the G·U reverse wobble but appears to be absent in the G25A·U20C double mutant (see the text). Panels B and C were generated with Pymol.⁵² (D) HDV ribozyme cleavage mechanism. C75 has a pK_a that is shifted toward neutrality and is in good position to serve as a general acid. The active site Mg²⁺ ion is positioned to activate the nucleophile. The identity of the functional group that accepts the proton from the 2′-OH of U(−1) is unknown, but candidates include a hydroxide from the solvent, a Mg²⁺-bound hydroxide, and the 2′-OH of G27. See Figure S5 of the Supporting Information for further details.

possible and may be mutually compatible with general base catalysis.^{14,15}

Metal ion catalysis is common in large ribozymes, including group I and group II introns, RNase P, and, likely, the spliceosome.^{16–20} The smaller, nucleolytic ribozymes can function in the absence of divalent cations, a characteristic that initially suggested metal ions may not play catalytic roles in their mechanism.²¹ However, there is significant evidence that a Mg²⁺ ion participates in the cleavage reaction of the HDV ribozyme under biologically relevant buffer conditions. For example, the rate–pH profile is inverted when Mg²⁺ is removed from the reaction mixture, suggesting a change in the reaction mechanism in the absence of metal ions.^{22–24} The catalytic metal ion has been estimated to contribute at least 25-fold to the rate of the HDV ribozyme cleavage step,²³ and similar values are estimated for the hammerhead ribozyme reaction.^{25,26}

Although the HDV ribozyme can function in the absence of divalent metal ions, under physiological buffer conditions, catalysis depends on the presence of divalent metal cations such as Mg²⁺.²⁷ These divalent cations both facilitate folding of the RNA and appear to participate in catalysis.^{23,28} A recent crystal structure resolved a Mg²⁺ ion within the active site of the HDV ribozyme.^{29,30} When the cleavage site dinucleotide was modeled into this crystal structure, the Mg²⁺ ion was observed to directly bind to the 2′-O of U(−1), which serves as the nucleophile, and to the *pro*-R_p oxygen of the scissile phosphate (Figure 1B). This suggested that the active site Mg²⁺ ion could act as a Lewis acid to activate the 2′-OH nucleophile and stabilize negative charge on the nonbridging oxygen of the scissile phosphate. Testing the functional relevance of this Mg²⁺ ion is especially important because the conformation of the HDV ribozyme cleavage site was not unambiguously determined by the electron density.²⁹

Although the solution biochemical experiments have suggested that a Mg²⁺ ion may play a direct role in the HDV ribozyme cleavage reaction, no data functionally linking the active site Mg²⁺ ion observed in the crystal structure to a role in the cleavage reaction are available. A phosphorothioate substitution at the *pro*-R_p oxygen of G1, a ligand to the active site Mg²⁺, is disruptive to catalysis.³¹ However, this modification was not rescued by a thiophilic metal ion, and thus, a functional interaction between the scissile phosphate and the active site Mg²⁺ ion has not yet been demonstrated.

The active site Mg²⁺ ion has additional interactions with the ribozyme. It forms a single inner-sphere ligand to the ribozyme core, the *pro*-S_p oxygen of U23. In addition, a rare but conserved reverse wobble pair, G25·U20, helps position this Mg²⁺ ion: atoms from this base pair serve as second-shell ligands that hydrogen bond to the hydration shell of the Mg²⁺ ion (Figure 1B). To address the question of whether the active site Mg²⁺ ion plays a catalytic role in the HDV ribozyme, we have characterized the effects of perturbing these outer-sphere ligands. The G25·U20 reverse wobble base pair was mutated to an isosteric A25·C20 base pair (Figure 1C). We find that this mutation is sufficient to disrupt binding of the active site Mg²⁺ ion and that the cleavage reaction of the A25·C20 double mutant uses a Mg²⁺-free mechanism. These findings suggest that the active site Mg²⁺ ion observed in the crystal structure plays a direct role in the cleavage reaction of the WT HDV ribozyme.

MATERIALS AND METHODS

RNA Preparation. The 74-nucleotide *trans*-acting HDV ribozyme was designed on the basis of a fast-folding version whose crystal structure has been determined trapped in the precleavage state.²⁹ A 63-nucleotide RNA (termed the “ribozyme strand”) was made by large-scale *in vitro* transcription and purified by urea denaturing gel electrophoresis as

previously described.²⁹ A 5'-Dy547-labeled 11-nucleotide fluorescent RNA (termed the "substrate strand") was prepared by chemical synthesis. The sequence of this strand is 5'-(DY547)-UAAU*GCGUUGCA, where the asterisk indicates the cleavage site. The substrate strand was purchased from Thermo Scientific, deprotected, and desalted by following the manufacturer's protocols.

Ribozyme Kinetics and Data Fitting. Rate constants for ribozyme reactions were obtained using single-turnover cleavage assays. In these, the ribozyme and DY547-tagged substrate RNAs were mixed to achieve final concentrations of 5 μ M ribozyme and 50 nM substrate in the indicated buffer (50 mM) in a total volume of 100 μ L. The buffers were potassium acetate (pH 5.0 and 5.5), potassium MES (pH 6.0 and 6.5), potassium MOPS (pH 7.0), and Tris-HCl (pH 7.5). The reaction mixture was heated at 90 °C for 2 min, cooled to room temperature for 10 min, and equilibrated at 37 °C for 2 min before a 5 μ L aliquot was removed to serve as the zero time point. The ribozyme reaction was initiated by adding sufficient concentrated MgCl₂ solutions, buffered with one of the buffers (50 mM) described above, to bring the reaction mixture to the desired final MgCl₂ concentration. At appropriate time points, a 5 μ L sample was removed and the reaction quenched with a 5–25 μ L volume of quenching buffer containing 5–200 mM EDTA and 57–90% formamide. Volumes were chosen such that the final concentration of EDTA was 2–10 times greater than the free Mg²⁺ concentration, ensuring that the reaction was terminated by the addition of the quenching buffer. Samples were immediately placed on ice and stored at –20 °C before they were analyzed on a 10% acrylamide, 7 M urea denaturing gel. Identical results were obtained when samples were placed on dry ice and stored at –80 °C. The fluorescent signal from the DY547 fluorophore was detected with a Typhoon 8600 variable mode imager (Molecular Dynamics) and quantified with ImageQuant 5.1 (Molecular Dynamics). Plots of fraction cleaved as a function of time were analyzed using KaleidaGraph 4.1 (Synergy Software).

The DY547 fluorophore is bulky and carries a positive charge. As a result, the labeled three-nucleotide product migrates more slowly in the polyacrylamide gel than the full-length substrate. To verify that the product was the expected length and contained a 2',3'-cyclic phosphate, the product was treated with T4 polynucleotide kinase and calf intestinal phosphatase and found to comigrate with an authentic DY547-UAAU RNA standard (Figure S1 of the Supporting Information).

Reactions were fit either to a single-exponential (eq 1) or to a double-exponential (eq 2) reaction as appropriate from the observed data. When reactions were fit to a double-exponential equation, the rate constant of the predominant, fast-reacting phase was used to calculate the kinetic and thermodynamic parameters described below.

$$F_t = F_0 + (F_\infty - F_0)(1 - e^{-k_{\text{obs}}t}) \quad (1)$$

$$F_t = F_0 + (F_\infty - F_0)[1 - f_1 e^{-k_{\text{obs},1}t} - (1 - f_1)e^{-k_{\text{obs},2}t}] \quad (2)$$

where F_t is the fraction of ribozyme cleaved at time t , F_0 is the fraction cleaved at time zero, F_∞ is the fraction cleaved at infinite time, and k_{obs} is the observed first-order rate constant; for a double-exponential process (eq 2), $f_1(F_\infty - F_0)$ is the fraction cleaved in an initial fast phase with a rate constant $k_{\text{obs},1}$ and $(1 - f_1)(F_\infty - F_0)$ is the fraction cleaved in a second slow

phase with a rate constant $k_{\text{obs},2}$. For Mg²⁺ titration studies, values as a function of Mg²⁺ concentration were fit to

$$k_{\text{obs}} = k_{\text{max}} \frac{([\text{Mg}^{2+}]/K_{\text{D,Mg}^{2+}})^{n_{\text{Hill}}}}{1 + ([\text{Mg}^{2+}]/K_{\text{D,Mg}^{2+}})^{n_{\text{Hill}}}} \quad (3)$$

where $K_{\text{D,Mg}^{2+}}$ is the apparent dissociation constant, k_{max} is the maximal observed rate constant, and n_{Hill} is the Hill coefficient for Mg²⁺ binding. For the rate–pH profile of the WT HDV ribozyme, the observed pK_a value was given by

$$k_{\text{obs}} = \frac{k_{\text{max}}}{1 + 10^{pK_a - \text{pH}}} \quad (4)$$

For the AC variant, the observed pK_{a1} and pK_{a2} values were obtained via

$$k_{\text{obs}} = k_{\text{max}} / (1 + 10^{pK_{a1} - \text{pH}} + 10^{\text{pH} - pK_{a2}} + 10^{pK_{a1} - pK_{a2}}) \quad (5)$$

Molecular Dynamics. We computed molecular dynamics (MD) trajectories starting with coordinates based on the structure of the HDV ribozyme trapped prior to cleavage (Protein Data Bank entry 3NKB), as previously described.²⁹ The 2'-H of the deoxynucleotides at positions 1 and 2 were replaced by 2'-OH to convert them to the corresponding ribonucleotides. The G25A and U20C mutations were created in silico using Accelrys Discover Studio Visualizer 2.0, followed by optimization of only the A25-C20 reverse wobble base pair, with the remainder of the ribozyme fixed. For the MD studies, C75 was protonated at the N3 position to represent the active state for general acid catalysis, and C41 was protonated at N3 to maintain the structural integrity of a C-protonated base triple.^{32–35} The partial charges used for the protonated cytosines were derived using the RESP method,³⁶ as described previously.³⁷ The ribozyme was solvated in an orthorhombic box of rigid TIP3P waters³⁸ with periodic boundary conditions. The system was neutralized with Na⁺ ions, and 0.15 M NaCl was added to the solvent to give a physiologically meaningful ionic strength. The solvation procedure was conducted using Maestro (Schrödinger, New York, NY). Details regarding the equilibration and simulation protocol used for the system have been described previously.^{37,39} Molecular dynamics simulations were performed with the Desmond MD program (D. E. Shaw Research, New York, NY) using the AMBER99 force field.⁴⁰ At least two independent 25 ns trajectories were propagated at 298 K in the canonical ensemble (i.e., at constant NVT) for each case studied.

Electrostatics Calculations. Electrostatic potential calculations were performed using the Adaptive Poisson-Boltzmann Solver (APBS),⁴¹ which uses the Finite Element ToolKit^{41–43} to solve the nonlinear Poisson–Boltzmann (NLPB) equations numerically. Structural coordinates were obtained from the starting structure of the ribozyme used for the MD simulations. All water molecules and crystallographic metal ions, except the metal ion at the catalytic site when specified, were omitted from the NLPB calculations, and C75 was left unprotonated; these settings allow the extent of the negative potential to be sensed and are customary for such calculations.^{23,44–46} In addition, C41, which is distal from the active site, was protonated as in the MD studies to maintain the aforementioned base triple.³⁵ Charges on C75 and C41 are identical to those used in our earlier electrostatics calculations.³⁷ The atomic radii and partial charges were defined using the AMBER99 parameter set,

except for protonated C41, for which the partial charges were derived using RESP calculations as described previously.³⁵

The following parameters of the electrostatics calculations were chosen to be consistent with similar previous calculations.^{45,47,48} The interior dielectric constant of the ribozyme was set to 2, a value previously shown to be physically meaningful,⁴⁹ and the solvent dielectric constant was set to 80. All calculations were performed on a grid centered on the crystal coordinates of the catalytic metal ion with a grid spacing of 0.35 Å. The dimensions of the ribozyme, centered on the position of the catalytic metal ion, were calculated in the X, Y, and Z directions, and the final grid dimensions were chosen after leaving a 20 Å distance between the ribozyme boundary and the grid boundary. A 2.0 Å exclusion radius was added to the ribozyme surface to incorporate hydrated sodium ions. The calculations were performed in the absence of any salt in the bulk solvent, as well as in the presence of different concentrations of mixed 1:1 and 2:1 salts, i.e., mixture of NaCl and MgCl₂, as described previously.⁴⁵ The radius of the catalytic Mg²⁺ or Na⁺ ion was set to 1.45 or 1.68 Å, respectively, each of which was shown previously to reproduce the corresponding experimental hydration free energy.^{50,51} The trends in the relative electrostatic binding free energies were maintained over a range of physically reasonable radii.

To estimate the binding energy of the metal ion at the reverse wobble, we adopted the methodology of Misra and Draper.⁵¹ We considered the cases of the WT and the G25A·U20C double mutant structures, with a single metal ion, either Mg²⁺ or Na⁺, located at the crystallographic position of the Mg²⁺ at the reverse wobble. The metal ion binding free energy is calculated from the difference between the total electrostatic free energy of the metal ion-bound ribozyme in solution and the sum of the total electrostatic free energies of the isolated ribozyme and the isolated metal ion in solution.

$$\Delta G_{\text{bind}}^{\text{el}} = \Delta G^{\text{el}}(\text{HDV} + \text{ion}) - [\Delta G^{\text{el}}(\text{HDV}) + \Delta G^{\text{el}}(\text{ion})] \quad (6)$$

The difference between $\Delta G_{\text{bind}}^{\text{el}}$ of the WT and G25A·U20C double mutant structures, as indicated in eq 7, provides an indication of the relative favorability of metal ion binding at the reverse G·U wobble in comparison to the reverse A·C wobble:

$$\Delta \Delta G_{\text{bind}}^{\text{el}} = \Delta G_{\text{bind}}^{\text{el}}(\text{WT}) - \Delta G_{\text{bind}}^{\text{el}}(\text{DM}) \quad (7)$$

Note that the site-specific binding free energy of a metal ion binding to a particular construct includes additional contributions to those given in eq 6, as discussed by Draper,⁵¹ but these contributions, as well as $\Delta G^{\text{el}}(\text{ion})$, will cancel for the calculation of $\Delta \Delta G_{\text{bind}}^{\text{el}}$ in eq 7.

We emphasize that these electrostatics calculations provide only qualitative information and are based on several approximations. For example, no conformational sampling of the ribozyme is included and no explicit water molecules are included (i.e., the ligation of water molecules to the Mg²⁺ is neglected), and for calculations involving Na⁺, the Na⁺ ion in the WT and G25A·U20C double mutant is assumed to be located at the same position as the Mg²⁺. Moreover, we found that the quantitative results depend on the dielectric constant and the ionic radii, although the trends in $\Delta \Delta G_{\text{bind}}^{\text{el}}$ between WT and the G25A·U20C double mutant can be reproduced within the physically reasonable regimes for these parameters.

The electrostatic potentials were rendered using PYMOL.⁵² The dxmath tool within APBS was used to obtain the difference between two electrostatic potential maps.

RESULTS

Here, we examine the impact of substituting the G25·U20 reverse wobble by mutating G25 to an adenine and U20 to a cytosine. This double mutant has the potential to allow formation of an A25·C20 reverse wobble base pair that is isosteric with a G·U reverse wobble (Figure 1B,C). Previous studies have tested the impact of single mutations of this G25·U20 base pair on ribozyme activity. At pH 8.0 and a saturating Mg²⁺ concentration, ~3000- and ~1600-fold reaction rate reductions were measured for the G25A single mutation of a genomic HDV ribozyme and the U23C single mutation of an antigenomic version (equivalent of U20 in the genomic ribozyme), respectively.^{53,54} These data suggest that the G25·U20 base pair is essential for ribozyme activity and that a reverse wobble conformation, rather than a Watson–Crick base pair, is required at this position. A double mutation would allow an isosteric reverse wobble to be adopted by an A25·C20 base pair.⁵⁵ While this base pair is similar in shape to a G·U reverse wobble pair, the presence of the N6 amino of adenosine in the minor groove is expected to alter the electrostatic properties of the binding site for the active site Mg²⁺. The G25A·U20C double mutant of the HDV ribozyme thus has the potential to specifically disrupt binding of the Mg²⁺ ion without perturbing the overall architecture of the ribozyme. We therefore characterized the G25A·U20C double mutant using solution biochemical and computational methods, in an effort to assess the role of the 25·20 base pair in binding the active site Mg²⁺ ion and to characterize the role of this ion in the chemical reaction.

The G25A·U20C Double Mutant of the HDV Ribozyme Retains an Active Structure. While an A·C base pair in the reverse wobble geometry is isosteric with a G·U reverse wobble base pair, the possibility exists that in the context of the HDV ribozyme an A25·C20 reverse wobble may not form stably. This would lead to structural changes at the active site. We therefore computed MD trajectories of the G25A·U20C double mutant. In these trajectories, Mg²⁺ ions present in the 3NKB crystal structure coordinates, including the ion at the reverse wobble, were retained. In our simulations, we found that the A25·C20 reverse wobble is stable over two independent 25 ns trajectories, with average A25(N1)–C20(N4) and A25(N6)–C20(N3) distances of 3.05 ± 0.19 and 2.90 ± 0.09 Å, respectively, consistent with hydrogen bonds (Table S1 of the Supporting Information). There were no noticeable conformational changes observed in the active site, including the general acid, C75, and the cleavage site dinucleotides G1 and U(–1) (data not shown).

In both of these trajectories, the active site Mg²⁺ ion remained bound to the A25·C20 reverse wobble, and the interaction of the metal ion with the A·C motif was found to be similar to its interaction with the reverse G·U wobble. As these simulations were much shorter than the time scale of the reaction, they may not address whether Mg²⁺ can stably bind to the G25A·U20C double mutant variant ribozyme. Limitations in both the molecular mechanical force field and the conformational sampling may prevent observation of any diffusion of the Mg²⁺ from this site. As the G25A·U20C double mutant has the potential to disrupt binding of the active

site Mg^{2+} , we next chose to explore the stability of the A25-C20 reverse wobble in the absence of this Mg^{2+} ion.

We ran three independent trajectories of the G25A-U20C double mutant ribozyme in the absence of Mg^{2+} at the active site (Figure 2). In two of the three trajectories, we found that a

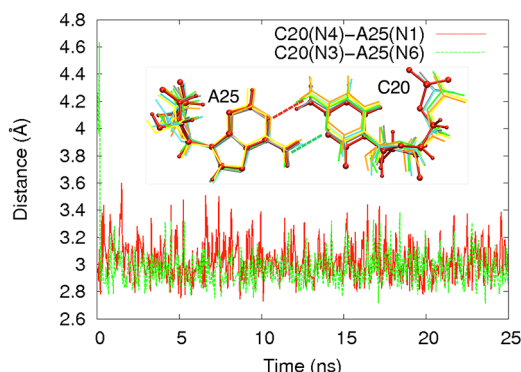


Figure 2. Stability of the A25-C20 reverse wobble along a MD trajectory. In this particular simulation, the active site Mg^{2+} ion was removed, and two Na^+ ions were placed in the bulk solvent. The C20(N4)–A25(N1) and C20(N3)–A25(N6) distances are plotted along the trajectory in red and green, respectively. The inset shows snapshots of the A-C reverse wobble at various time steps along the trajectory: red, 0 ns (also ball-and-stick representation); cyan, 5 ns; gray, 10 ns; orange, 15 ns; yellow, 20 ns; green, 25 ns. Very little motion of the A-C reverse wobble occurs.

Na^+ ion moves from bulk solution to the active site and that the A25-C20 reverse wobble and the active site are stable (Table S1 of the Supporting Information). In the third trajectory, no Na^+ ion moved into the region to bind to the reverse wobble, and one hydrogen bond in the A25-C20 reverse wobble was lost at ~ 2.5 ns. This observation probably resulted from starting the trajectory without any ion in this region, leading to breaking of the hydrogen bond before the Na^+ was able to move into the region to stabilize the reverse wobble. This situation is not likely relevant to the ribozyme in solution. Thus, we did not further analyze this trajectory. As shown in Table S1 of the Supporting Information, for the first two trajectories, the two hydrogen bonds in the A25-C20 reverse wobble have distances similar to those in the presence of bound Mg^{2+} .

Overall, these results suggest that the structure of the G25A-U20C double mutant of the HDV ribozyme is stable in the presence or absence of a Mg^{2+} ion in the active site. However, monovalent ions may be required to stabilize the geometry of the A25-C20 wobble in the absence of Mg^{2+} ions.

The A25-C20 Variant of the HDV Ribozyme Is Catalytically Active. Our computational studies suggested that the G25A-U20C double mutant of the HDV ribozyme

would fold correctly. Therefore, we introduced a G25A-U20C double mutation into the HDV ribozyme. The sequences of the WT ribozyme and the G25A-U20C double mutant were derived from the ribozyme whose structure we had recently determined.²⁹ This is a two-piece RNA containing a large RNA strand that spans most of the active site and is formally a ribozyme. A small substrate RNA was annealed to this ribozyme to reconstitute the three-dimensional structure prior to initiation of the reaction with Mg^{2+} . For this study, a fluorophore, DY547, was linked to the 5'-end of the substrate. Upon incubation with ribozyme, this substrate is cleaved to generate the expected products (Figure S1 of the Supporting Information). We would predict that this modification would not affect catalysis because the crystal structure of this RNA reveals a sharp turn at the scissile phosphate that places the nucleotides upstream of U(–1) out of the active site and into bulk solution.²⁹ We find that the single-turnover kinetic parameters k_{max} , $K_{\text{D,Mg}^{2+}}$, and n_{Hill} obtained in this study are similar to those obtained with a radiolabeled substrate lacking the fluorophore (Table 1).⁵⁶

Next, we conducted single-turnover studies of the AC variant. These studies demonstrated that, at $\text{pH} \leq 7$, the observed rate constant (k_{obs}) of the AC variant is at most ~ 100 -fold lower than that of the WT (Figures 3 and 4). Thus, the G25A-U20C double mutation partially rescued the activity lost in the single mutations. In these reactions, the G25A-U20C variant cleaved its substrate monophasically to at least 80% of completion [Figure 3A (\blacktriangle)]. This extent of the reaction is similar to what is observed with the WT ribozyme [Figure 3A (\blacksquare)] and suggests that the majority of the AC variant is in an active conformation. Recently, Perrault and co-workers described a similar finding for the antigenomic ribozyme.⁵⁷

The G25A-U20C Double Mutation Does Not Affect the Apparent Mg^{2+} Ion Binding Properties. To further examine the folding properties of the G25A-U20C double mutant, Mg^{2+} titrations were conducted with both the WT and G25A-U20C double mutant ribozyme. At every Mg^{2+} concentration tested, the reaction rate of the G25A-U20C double mutant decreased by 80–120-fold relative to that of the WT (Figure 3). As a result, the apparent $K_{\text{D,Mg}^{2+}}$ value is the same, within error, for both the G25A-U20C double mutant and the WT ribozymes. We observed apparent $K_{\text{D,Mg}^{2+}}$ values of 1.4 ± 0.1 and 1.3 ± 0.1 mM for the G25A-U20C double mutant and WT ribozymes, respectively (Table 1). In addition, the Hill coefficient, n_{Hill} , does not change as a result of the mutation (1.8 ± 0.2 for the WT vs 2.0 ± 0.2 for the mutant) (Table 1). This similarity suggests that the same concentration of Mg^{2+} ion is needed to attain a folded conformation and that the decreased activity of the G25A-U20C double mutant is most likely not caused by misfolding.

Table 1. Kinetic Parameters for Cleavage of WT and Double Mutant Ribozymes

	k_{max} (min^{-1})	$K_{\text{D,Mg}^{2+}}$ (mM)	n_{Hill}	$\text{p}K_{\text{a}}$
WT (fluorophore)	6.2 ± 0.2^a	1.3 ± 0.1^a	1.8 ± 0.2^a	6.1 ± 0.1^b
WT (radiolabel)	7.0 ± 0.2^c	2.1 ± 0.1^c	1.6 ± 0.1^c	6.4^d
A25-C20 (fluorophore)	0.078 ± 0.002^a	1.4 ± 0.1^a	2.0 ± 0.2^a	6.2 ± 0.2^b

^aReported here. Reactions were performed at 37 °C in 50 mM potassium MOPS (pH 7.0). ^bReported here. Reactions of WT (fluorophore) and A25-C20 (fluorophore) were performed in 5 and 50 mM Mg^{2+} , respectively, at 37 °C. The buffers were potassium acetate (pH 5.0 and 5.5), potassium MES (pH 6.0 and 6.5), potassium MOPS (pH 7.0), and Tris-HCl (pH 7.5). All were at a concentration of 50 mM. ^cValues from ref 56. In 25 mM Tris-HCl (pH 7.0) at 37 °C. ^dValues from ref 22. In 5 mM Mg^{2+} . The buffer was 25 mM MES (pH 4.5–6.5) or 25 mM Hepes (pH 6.75–9.0).

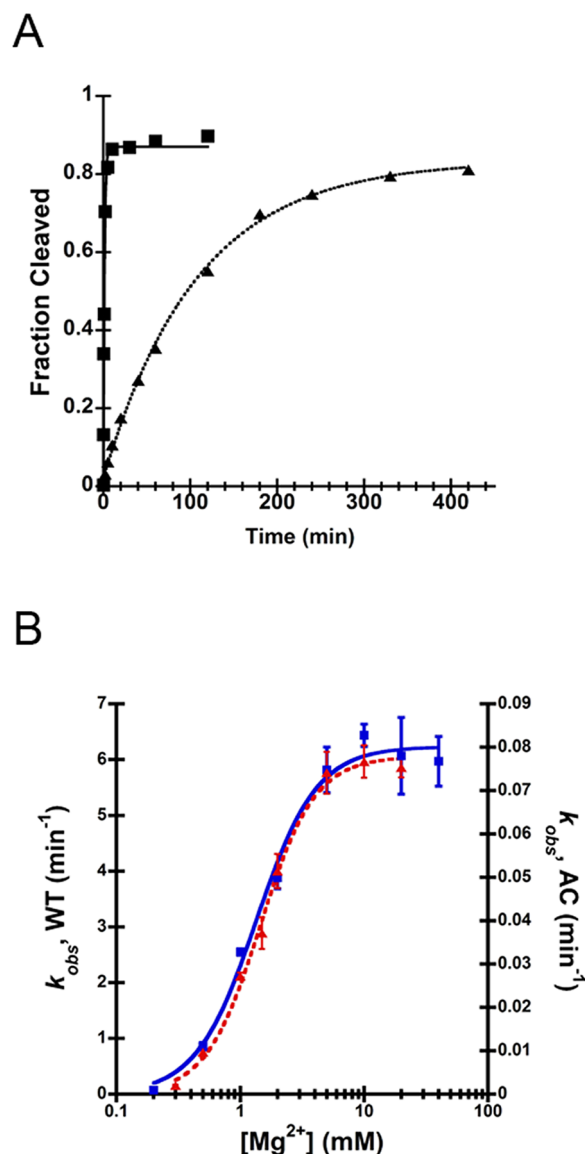


Figure 3. Magnesium dependence of the HDV ribozyme reaction. (A) Comparison of the WT and A25-C20 double mutant ribozymes. Cleavage of a fluorescently labeled RNA substrate by WT (■) and A25-C20 double mutant (▲) ribozymes. Cleavage reaction mixtures contained 0.5 mM Mg^{2+} and 50 mM MOPS (pH 7.0). (B) Cleavage rate constants as a function of Mg^{2+} concentration. Rate constants for WT (blue ■) and A25-C20 double mutant (red ▲) ribozymes are plotted as a function of Mg^{2+} ion concentration. All reaction mixtures contained 50 mM MOPS (pH 7.0). Although the maximal velocity is higher for the WT ribozyme than the A25-C20 double mutant ribozyme, the apparent $K_{D,Mg^{2+}}$ and n_{Hill} are the same for the two ribozymes within error (Table 1).

The G25A-U20C Double Mutant in the Presence of Mg^{2+} Has the Same Rate-pH Profile as the WT Ribozyme in the Absence of Mg^{2+} . To assess the impact of the G25A-U20C double mutation on active site folding and catalysis, we characterized the rate-pH profile of this variant. We first determined the rate-pH profile for this WT ribozyme in 5 mM Mg^{2+} , and we obtained the expected profile with a log-linear increase in rate between pH 5.0 and 6.0 and a pK_a of 6.1 ± 0.1 [Figure 4 (■)]. This is in good agreement with the pK_a previously determined using a radiolabeled oligonucleotide of 6.4 under similar conditions.²²

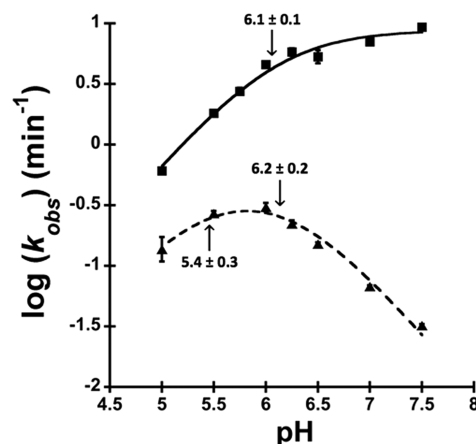


Figure 4. pH-rate profiles of the A25-C20 double mutant ribozyme as compared to that of the WT. The reactions were performed in 5 mM Mg^{2+} for the WT (■) and 50 mM Mg^{2+} for the A25-C20 double mutant (▲). The curves were fit by using eq 4 for the WT and eq 5 for the A25-C20 double mutant ribozyme. The apparent pK_a values are indicated with an arrow and summarized in Table 1. Note that the apparent pK_a of 5.4 ± 0.3 might originate from acid denaturation or could be due to a contribution of a catalytic metal ion only at low pH (see Discussion).

The rate-pH profile of the G25A-U20C double mutant was studied in 50 mM Mg^{2+} , well above the apparent $K_{D,Mg^{2+}}$ for this ribozyme (Figure 3B). We found that the reaction is nearly independent of pH in the pH range of 5.5–6.0 [Figure 4 (▲)], likely because the general acid, C75, remains largely protonated in this pH range.

If the active site were misfolded and a structural rearrangement were the rate-limiting step for the G25A-U20C double mutant, then the change in k_{obs} as a function of pH might be minimal. However, at pH >6.0, the reaction rate decreases log-linearly, suggesting that chemistry, not folding, is rate-limiting and that the cleavage reaction rate is dominated by deprotonation of C75 (Figure 4). The apparent pK_a value is 6.2 ± 0.2 under these conditions and, as discussed below, likely represents the pK_a of C75. We observed that the cleavage rate decreases by ~2-fold when the pH is decreased below 5.0. Loss of activity at low pH may be due to acid denaturation and might suggest that the G25A-U20C double mutant is less stable than the WT ribozyme as both A and C start to become protonated in this pH range.⁵⁸ Such a protonation at A25 might allow the formation of a positively charged standard A·C wobble between A25 and C20. This conformation is not isosteric with a reverse wobble and would be predicted to be disruptive to the ribozyme's active site structure. Another possibility is a slight contribution from a general base with a pK_a near 5.4 or that is lost near this pH (see Discussion).

The rate-pH profile of the G25A-U20C double mutant is inverted from that of the WT ribozyme in Mg^{2+} -containing buffers (in Figure 4, compare triangles and squares). Qualitatively, it resembles the rate-pH profile of the WT ribozyme reacting in the absence of Mg^{2+} .^{22,23} The data for the WT ribozyme were interpreted to suggest that a Mg^{2+} -dependent proton transfer is involved in the cleavage reaction under biologically relevant, Mg^{2+} -containing conditions.²⁴ In an effort to restore a WT-like pH-rate profile, we repeated these experiments in 500 mM Mg^{2+} . However, these data are not significantly different from the data obtained in 50 mM Mg^{2+} (not shown), suggesting that the active site Mg^{2+} binds

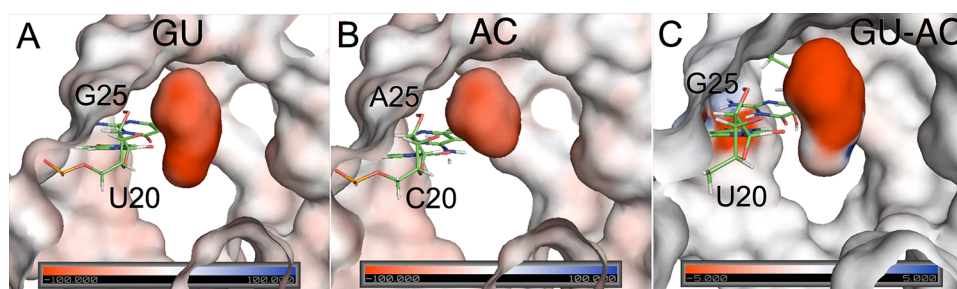


Figure 5. Surface electrostatic potential of the precleaved HDV ribozyme. (A) WT structure and (B) G25A-U20C double mutant, labeled AC. (C) Difference map showing changes in the electrostatic potential between the WT and G25A-U20C double mutant ribozymes mapped onto the WT structure. The scale for panels A and B is -100 to 100 kT/e and for panel C is -5 to 5 kT/e. The pocket near the G-U reverse wobble in the WT structure is more negative than the pocket near the A-C reverse wobble in the G25A-U20C double mutant structure. Panels were rendered using Pymol.⁵²

especially weakly or in an alternate binding pocket within the G25A-U20C double mutant.

The G25A-U20C Double Mutant in the Absence of Mg^{2+} Has the Same Rate-pH Profile as the WT Ribozyme in the Absence of Mg^{2+} . As the G25A-U20C double mutant rate-pH profile in the presence of Mg^{2+} appeared to resemble the rate-pH profile of the WT HDV ribozyme in the absence of Mg^{2+} , we wanted to compare the reaction of both ribozymes in the absence of Mg^{2+} . Unfortunately, the two-piece HDV ribozyme used here does not react in the absence of Mg^{2+} , possibly because the substrate does not stably anneal to the ribozyme at the high NaCl concentration used in these reactions. We therefore introduced the G25A-U20C double mutation into a *cis*-acting, self-cleaving version of the HDV ribozyme characterized previously.⁵⁹ This allowed a side-by-side comparison of the WT ribozyme and G25A-U20C double mutant in the absence of Mg^{2+} ion (Supporting Information).

We first studied the pH dependence of the G25A-U20C double mutant reaction in the absence of divalent metal ions (see the Supporting Information and Materials and Methods). These reactions were performed at 1 M NaCl, and 100 mM EDTA (final concentration) was included in the reaction buffer to chelate any trace amount of contaminating polyvalent metal ions, especially at low pH (see Supporting Information). We observed that the G25A-U20C double mutant was catalytically active under all the pH conditions tested (Figure S2 of the Supporting Information). At least 80% of completion was achieved in all but the reaction at pH 8.0. The reaction progress can be fit to eq 1. This suggests that the Mg^{2+} ion is nonessential to the G25A-U20C double mutant catalysis when a high concentration of monovalent salt is present. The reaction is pH-independent between pH 6.0 and 6.5, and an inhibitory effect is seen below pH 6.0 (Figure S3 of the Supporting Information). The rate-pH curve yields an apparent pK_a of 7.3 ± 0.1 , which is assigned to general acid C75.

We next compared the rate-pH profile of the one-piece WT HDV ribozyme in the absence of divalent metal ions to that obtained for the G25A-U20C double mutant. The rate-pH profile is bell-shaped, which suggests the involvement of two ionizable groups (Figure S3 of the Supporting Information). Two apparent pK_a values were obtained from the rate-pH profile. The log-linear decrease in reaction rate between pH 7.5 and 8.5 is attributed to the deprotonation of general acid C75 as discussed elsewhere in this study. Thus, the high pK_a value of 7.6 ± 0.1 likely represents the pK_a of C75, similar to that obtained with the double mutant. Between pH 6.0 and 6.5,

the reaction rate is largely independent of pH, which is consistent with the fact that a constant amount of the functional form of C75 is present over this pH range. An apparent pK_a value of 5.3 ± 0.2 was also obtained, similar to what is observed with the one-piece (Figure S3 of the Supporting Information) and the two-piece G25A-U20C double mutant HDV ribozymes (Figure 4). In general, the rates and shape of the curve agree well with those previously reported.²³

Comparing the two rate-pH profiles (Figure S3 of the Supporting Information), we observed that the G25A-U20C double mutant reaction shows a pH dependence similar to that of the WT ribozyme. A log-linear decrease at high pH range is almost parallel to that observed in the WT ribozyme. The reaction rate of the G25A-U20C double mutant is only ~ 5 -fold slower than that of the WT under the same reaction condition without divalent ions, which corresponds to a ΔG°_{37} of just 1 kcal/mol. This indicates that the G25A-U20C double mutant is only slightly less active than the WT. The ~ 5 -fold rate difference observed here, in Mg^{2+} -free buffers, is also observed when Mg^{2+} -mediated base catalysis is minimal at pH 5.0 (Figure 4), suggesting that folding of the G25A-U20C double mutant ribozyme is largely intact in the presence and absence of Mg^{2+} (Figure 4).

Electrostatics of the Active Site Are Affected by the G25A-U20C Double Mutation. Because the solution biochemical studies strongly suggested that the G25A-U20C double mutant was not able to bind the active site Mg^{2+} , we sought to characterize the electrostatics of the active site. MD simulations can be a useful tool for understanding important motions in biological systems; however, there are known limitations associated with MD for investigating interactions between divalent metal ions and macromolecules. These limitations include the inadequate description of divalent ions by molecular mechanical force fields and issues related to trapping in local minima caused by insufficient sampling during simulations.^{60,61} We therefore performed NLPB electrostatics calculations on the WT and G25A-U20C double mutant structures to obtain qualitative insight into the metal ion binding at the G-U and A-C reverse wobbles, respectively. For both ribozymes, an intense negative surface is found in the vicinity of the reverse wobble (Figure 5), similar to that reported previously.³⁷ To directly compare the results from the WT and G25A-U20C double mutant ribozymes, we calculated a surface electrostatic difference plot (G-U electrostatic surface minus A-C electrostatic surface). This plot clearly reveals a negative patch in the vicinity of the reverse wobble (Figure

5C), indicating that the metal ion binding pocket near the A-C reverse wobble is less negatively charged and suggesting weaker binding of the metal ion at the A-C reverse wobble. These observations are consistent with the changes in the rate–pH profile we observed in the G25A·U20C double mutant ribozyme.

We also estimated the relative binding free energy for binding of the metal ion to the catalytic sites of the WT and variant ribozymes using eqs 6 and 7. These calculations were performed for either a Mg^{2+} or a Na^+ ion binding to the catalytic site. Negative values for $\Delta\Delta G_{bind}^{el}$ were found, indicating that metal ion binding at this site is more thermodynamically favorable for the WT than for the G25A·U20C double mutant ribozyme, as expected from the NLPB electrostatic surface potentials in Figure 5. In particular, for a Mg^{2+} ion and a dielectric constant of 2, the binding is predicted to be ~ 12 kcal/mol more favored at the WT G·U reverse wobble than at the A-C reverse wobble of the double mutant. Likewise, binding of Na^+ ion in the active site of the WT ribozyme is ~ 5 kcal/mol more favored than in the active site of the double mutant. It is important to note, however, that these values are only qualitative and are not quantitatively accurate (e.g., the magnitude of these differences decreases with the choice of a higher dielectric constant). The lower magnitude of $\Delta\Delta G_{bind}^{el}$ for Na^+ suggests that the metal binding pocket at the G·U reverse wobble is more selective toward Mg^{2+} ions, consistent with the experiments described above. The results were similar for calculations in the presence of varying concentrations of diffuse 1:1 and 2:1 salts (data not shown).

DISCUSSION

The HDV ribozyme uses a rare G·U reverse wobble pair to help position an active site Mg^{2+} ion. Hydrated Mg^{2+} ions have long been known to interact with the negative dipoles of canonical G·U base pairs.^{62,63} However, these interactions are typically in the major groove, which in the case of A-form RNA is deep and inaccessible; such Mg^{2+} ions are thus unlikely to be catalytic. In contrast, the active site Mg^{2+} ion of the HDV ribozyme is in the minor groove and is therefore in excellent position to participate in the cleavage reaction. This can occur because the G25·U20 reverse wobble has G25 in the *syn* geometry, allowing N7 and O6 of the G to reside in the shallow and accessible minor groove. G25 is thus able to help position the active site Mg^{2+} ion in such a way that it could participate in catalysis. In this study, we assessed the catalytic potential of this ion using functional assays.

The G25A·U20C Double Mutation Does Not Disrupt the Structure of the HDV Ribozyme. The G25·U20 reverse wobble pair of the HDV ribozyme contributes significantly to the stability of the active site Mg^{2+} ion by providing outer-sphere ligands and by enhancing the magnitude of the negative charge in the metal ion binding pocket.^{29,37} An A-C reverse wobble base pair is isosteric with the G·U reverse wobble but substitutes the carbonyl on the binding face with an amino group.⁵⁵ In this manner, this double mutation has the potential to disrupt active site metal ion binding without perturbing the tertiary structure of the RNA.

Upon introduction of mutations into RNA molecules, it is possible to generate RNA molecules that are misfolded into noncatalytic conformations. There are several pieces of evidence, however, suggesting that the G25A·U20C double mutant is not misfolded. First, under single-turnover con-

ditions, the mutant ribozyme reacts with monophasic kinetics and to $\sim 80\%$ completion, similar to the WT ribozyme (Figure 3). Such behavior is expected of a single population of ribozymes reacting in a similar manner. Second, characterization of the rate–pH profile for the G25A·U20C double mutant suggests that chemistry, not folding, is rate-limiting. If a conformational change were the rate-limiting step, we would expect to see a profile that was largely independent of pH. Instead, we observe a profile in which the rate constant decreases in a log–linear fashion above pH ~ 6.0 (Figure 4). Third, the Mg^{2+} –rate profile of the G25A·U20C double mutant is strikingly similar to that of the WT ribozyme, with respect to both the apparent $K_{D,Mg^{2+}}$ and the Hill coefficient, n_{Hill} (Figure 3). This suggests that the tertiary structure forms similarly, that the metal ions contributing to the three-dimensional structure bind with similar affinity, and that the thermodynamics of RNA folding are largely unaffected by this mutation.

The lack of structural disruption in the double mutant is also supported by the calculations. In molecular dynamics simulations of the G25A·U20C double mutant, the A25·C20 reverse wobble remains largely intact, even in the absence of Mg^{2+} . In addition, the key active site nucleotides, including general acid C75 and cleavage sites G1 and U(–1), are largely unperturbed. This is consistent with the biochemical experiments, strongly suggesting that the structure of the HDV ribozyme is not significantly changed in the G25A·U20C double mutant.

Lastly, we note that when the pH was decreased to 5, the difference in rate constants between the WT ribozyme and the G25A·U20C double mutant ribozyme is lessened. In fact, when the plateau region of the rate–pH profile of the AC variant is extrapolated to pH 4.5, where the Mg^{2+} -dependent deprotonation in the WT ribozyme hardly contributes, similar rate constants are obtained for the WT and G25A·U20C double mutant (Figure 4). This observation further supports native folding of the G25A·U20C double mutant.

The G25A·U20C Double Mutant Disrupts Binding of the Active Site Mg^{2+} Ion. The rate–pH profile of the WT HDV ribozyme depends critically on the presence of Mg^{2+} ions. In the presence of Mg^{2+} ions, the rate constant increases log–linearly with pH until pH ~ 6 where it plateaus [Figure 4 (■)]. When the Mg^{2+} ions are removed from the reaction mixture, the pH–rate profile is inverted [Figure 4 (▲)]:^{22,24} it is flat until pH ~ 6 , where it decreases log–linearly with pH. This inversion is consistent with loss of a proton transfer with a pK_a of >10 and supports a mechanism in which C75 serves as the general acid and the base has a pK_a of 5.4 or lower or the transfer of a proton from the 2'-OH occurs in a non-rate-determining step (Figures S4 and S5 of the Supporting Information). (The general base with a pK_a of 5.4 seems unlikely as this is a low pK_a for a general base and also because the low-pH arm of the double mutant rate–pH profile could be due to acid denaturation or the contribution of a catalytic metal ion only at low pH.) As a result, the transfer of a proton from N3 of C75 to the 5'-hydroxyl leaving group represents the only pK_a that can be observed in this pH range in the absence of Mg^{2+} .

The rate–pH profile of the G25A·U20C double mutant in Mg^{2+} ion looks very much like that for a ribozyme that lacks or mispositions the active site Mg^{2+} ion.^{22,24} These reactions were performed at a Mg^{2+} ion concentration of 50 mM, well above the Mg^{2+} ion concentration in which the G25A·U20C double mutant achieves maximal velocity. Similar to the WT ribozyme

reaction rate in the absence of Mg^{2+} ions, the reaction rate of the G25A·U20C double mutant decreases with pH, suggesting that the Mg^{2+} -dependent proton transfer observed in the WT ribozyme is missing (Figures S4 and S5 of the Supporting Information). These data suggest that in the G25A·U20C double mutant, the interaction between the active site Mg^{2+} ion and the cleavage site is lost. Addition of Mg^{2+} at concentrations as high as 500 mM is not sufficient to restore the pH–rate profile to that seen in the WT ribozyme.

This model is supported by shifts in the pK_a of C75 observed in this study. The pK_a of C75 is dependent on the concentration of Mg^{2+} ion in the reaction buffer. As the concentration of Mg^{2+} is increased, the pK_a of C75 decreases.^{9,22} This anticooperativity suggests that one or more Mg^{2+} ions are bound in the active site of the WT HDV ribozyme close enough to C75 that the protonated base and the ion can interact electrostatically. This is consistent with the crystal structure of the HDV ribozyme in which N4 of C75 is within 3.5 Å of the hydration shell of the active site Mg^{2+} ion and may therefore serve as an outer-sphere ligand.²⁹ In the WT ribozyme, we observed that the pK_a of C75 is 6.1 ± 0.1 in the presence of 5 mM Mg^{2+} (Figure 4). In the G25A·U20C double mutant, however, this pK_a is not shifted lower when the Mg^{2+} concentration is increased to 50 mM. In our studies, pK_a values of 6.2 ± 0.2 are obtained for C75 (Figure 4). In contrast, Nakano et al. observed that the pK_a of C75 within the WT ribozyme shifted from 6.4 to 5.8 when the Mg^{2+} ion concentration was increased from 5 to 50 mM.²² This suggests that in the G25A·U20C double mutant the environment near C75 is less positively charged. Again, this is consistent with a model in which the active site Mg^{2+} ion no longer occupies the binding site observed in the crystal structure.

Electrostatics calculations further suggest that the G25A·U20C double mutant specifically disrupts active site Mg^{2+} ion binding. NLPB calculations reveal a significant loss of negative charge in the active site Mg^{2+} ion binding pocket in the double mutant (Figure 5). Furthermore, the $\Delta\Delta G$ between the WT and the G25A·U20C double mutant for Mg^{2+} binding is ~ 12 kcal/mol, suggesting that active site Mg^{2+} binding is more thermodynamically favorable to the WT than to the G25A·U20C double mutant. Note that the quantitative value for $\Delta\Delta G$ depends on certain choices of parameters, such as dielectric constant, but the sign of this quantity is reproducible.

These results all point to a scenario in which the active site Mg^{2+} ion in the G25A·U20C double mutant is displaced or altered such that it can no longer interact with the 2'-hydroxyl of U(−1) and C75 (Figures S4 and S5 of the Supporting Information). Overall, these data indicate that the active site Mg^{2+} ion observed in the crystal structure of the WT HDV ribozyme is indeed positioned at the reverse G·U wobble and appears to participate directly in catalysis.

The Mg^{2+} Binding Isotherm Does Not Reflect Binding of an Active Site Mg^{2+} Ion. The dependence of the attainment of maximal ribozyme activity on Mg^{2+} ion concentration is the same in both the WT and G25A·U20C double mutant ribozymes. Although the G25A·U20C double mutant never matches the velocity of the WT ribozyme, the apparent $K_{D,\text{Mg}^{2+}}$ and Hill coefficient are, within error, the same (Table 1). As the G25A·U20C double mutant appears to disrupt active site Mg^{2+} binding as discussed above, these data suggest that structural Mg^{2+} ion binding, not active site Mg^{2+} binding, dominates the apparent $K_{D,\text{Mg}^{2+}}$ and observed Hill coefficients. The catalytic Mg^{2+} ion must therefore have a

higher affinity than the structure-stabilizing Mg^{2+} ions. Consistent with this interpretation, high-affinity Mg^{2+} ion binding sites in RNAs are predicted to have dissociation constants in the range of 1–25 μM (depending on ionic strength).^{28,49}

What Is Activating the Nucleophile? If the G25A·U20C double mutant ribozyme lacks an active site Mg^{2+} ion, are there mechanisms by which this ribozyme could activate the 2'-hydroxyl nucleophile? There are several possibilities. First, there is a Na^+ ion-binding pocket in the ribozyme active site that is observed when crystals of the HDV ribozyme are soaked in buffers containing Na^+ ion.³⁷ While this Na^+ binding site partially overlaps the active site Mg^{2+} ion, its binding is distinct from that of the active site Mg^{2+} ion. The Na^+ ion interacts through its water ligands with nucleotides G27 and A77 of the ribozyme. This ion could facilitate the cleavage reaction through electrostatic effects, stabilizing the developing negative charge on the nucleophile and the scissile phosphate, but it is not in position to interact directly with the 2'-hydroxyl nucleophile or the scissile phosphate.

In both the WT ribozyme and the G25A·U20C double mutant, the acceptor of the proton from the 2'-hydroxyl of U(−1) in the cleavage reaction is unknown. There are several possibilities. The 2'-hydroxyl of U(−1) is hydrogen bonded to the 2'-hydroxyl of G27, and this hydrogen bond is likely to be retained in the G25A·U20C double mutant as the active site structure appears to remain intact. Alternatively, the proton acceptor could be a water or hydroxide from the surrounding solvent, which may not be detected in the double mutant if it occurs in a step that is not rate-determining. In the case of the WT ribozyme, one of the water ligands from the catalytic Mg^{2+} ion could serve this role. Thus, the active site Mg^{2+} ion could play two roles in the WT, interacting with the nucleophile as a Lewis acid, coordinating a hydroxide molecule to serve as a Brønsted base, or both (Figure S4 of the Supporting Information).

This study represents the first set of data to functionally link the active site Mg^{2+} ion observed in the HDV ribozyme active site to a catalytic role in the cleavage reaction. Key questions still remain, however. The identity of the high pK_a that affects the rate–pH profile in the WT ribozyme, but not in the G25A·U20C double mutant, is still unknown. It could arise from ionization of a water bound to the active site Mg^{2+} that is deprotonated to serve as a general base (Figure S5A of the Supporting Information), from hydroxide in solution, from the 2'-hydroxyl of G27 or from the pK_a of the 2'-hydroxyl of U(−1) itself (Figure S5B of the Supporting Information). In addition, while these data associate the G·U reverse wobble with the catalytic metal ion, contributions of other ligands, such as the *pro-R_p* oxygen of the scissile phosphate, to metal ion catalysis have not yet been evaluated.

■ ASSOCIATED CONTENT

● Supporting Information

Identification of the HDV ribozyme cleavage product (Figure S1), self-cleavage reaction of the G25A·U20C double mutant (Figure S2), pH–rate profiles for the self-cleavage reactions of the G25A·U20C double mutant and WT in the absence of Mg^{2+} ion (Figure S3), summary of population–pH profiles for generating observed rate–pH profiles (Figure S4), and possible mechanisms for deprotonation of the 2'-hydroxyl (Figure S5), and statistics from MD simulation of the G25A·U20C double

mutant (Table S1). This material is available free of charge via the Internet at <http://pubs.acs.org>.

AUTHOR INFORMATION

Corresponding Author

*B.L.G.: telephone, (765) 496-6165; fax, (765) 494-7897; e-mail, barbgolden@purdue.edu. P.C.B.: telephone, (814) 863-3812; fax, (814) 865-2927; e-mail, pcb5@psu.edu.

Present Address

^{||}Department of Chemistry, University of Illinois at Urbana-Champaign, Urbana, IL 61801.

Funding

This project was supported by National Institutes of Health (NIH) Grant R01GM095923 (B.L.G. and P.C.B.), NIH Grant GM56207 (S.H.-S.), the Purdue University Department of Biochemistry, the Markey Center for Structural Biology, and the Purdue University Center for Cancer Research (B.L.G.).

Notes

The authors declare no competing financial interest.

ACKNOWLEDGMENTS

We thank Pallavi Thaplyal and Aamir Mir for lively discussions and for helpful suggestions about the manuscript. The instrumentation was funded by National Science Foundation Grant OCI-0821527.

ABBREVIATIONS

HDV, hepatitis delta virus; MD, molecular dynamics; NLPB, nonlinear Poisson–Boltzmann; WT, wild-type.

REFERENCES

- (1) Perrotta, A. T., and Been, M. D. (1991) A pseudoknot-like structure required for efficient self-cleavage of hepatitis delta virus RNA. *Nature* 350, 434–436.
- (2) Ferre-D'Amare, A. R., Zhou, K. H., and Doudna, J. A. (1998) Crystal structure of a hepatitis delta virus ribozyme. *Nature* 395, 567–574.
- (3) Salehi-Ashtiani, K., Luptak, A., Litovchick, A., and Szostak, J. W. (2006) A genomewide search for ribozymes reveals an HDV-like sequence in the human CPEB3 gene. *Science* 313, 1788–1792.
- (4) Webb, C. H., Riccitelli, N. J., Ruminski, D. J., and Luptak, A. (2009) Widespread occurrence of self-cleaving ribozymes. *Science* 326, 953.
- (5) Eickbush, D. G., and Eickbush, T. H. (2010) R2 retrotransposons encode a self-cleaving ribozyme for processing from an rRNA cotranscript. *Mol. Cell. Biol.* 30, 3142–3150.
- (6) Webb, C. H., and Luptak, A. (2011) HDV-like self-cleaving ribozymes. *RNA Biol.* 8, 719–727.
- (7) Ruminski, D. J., Webb, C. H., Riccitelli, N. J., and Luptak, A. (2011) Processing and translation initiation of non-long terminal repeat retrotransposons by hepatitis delta virus (HDV)-like self-cleaving ribozymes. *J. Biol. Chem.* 286, 41286–41295.
- (8) Bevilacqua, P. C., and Yajima, R. (2006) Nucleobase catalysis in ribozyme mechanism. *Curr. Opin. Chem. Biol.* 10, 455–464.
- (9) Gong, B., Chen, J. H., Chase, E., Chadalavada, D. M., Yajima, R., Golden, B. L., Bevilacqua, P. C., and Carey, P. R. (2007) Direct measurement of a pK_a near neutrality for the catalytic cytosine in the genomic HDV ribozyme using Raman crystallography. *J. Am. Chem. Soc.* 129, 13335–13342.
- (10) Guo, M., Spitale, R. C., Volpini, R., Krucinska, J., Cristalli, G., Carey, P. R., and Wedekind, J. E. (2009) Direct Raman measurement of an elevated base pK_a in the active site of a small ribozyme in a precatalytic conformation. *J. Am. Chem. Soc.* 131, 12908–12909.

- (11) Rupert, P. B., and Ferre-D'Amare, A. R. (2001) Crystal structure of a hairpin ribozyme-inhibitor complex with implications for catalysis. *Nature* 410, 780–786.
- (12) Martick, M., and Scott, W. G. (2006) Tertiary contacts distant from the active site prime a ribozyme for catalysis. *Cell* 126, 309–320.
- (13) Wilson, T. J., and Lilley, D. M. (2011) Do the hairpin and VS ribozymes share a common catalytic mechanism based on general acid-base catalysis? A critical assessment of available experimental data. *RNA* 17, 213–221.
- (14) Liu, L., Cottrell, J. W., Scott, L. G., and Fedor, M. J. (2009) Direct measurement of the ionization state of an essential guanine in the hairpin ribozyme. *Nat. Chem. Biol.* 5, 351–357.
- (15) Viladoms, J., Scott, L. G., and Fedor, M. J. (2011) An active-site guanine participates in glmS ribozyme catalysis in its protonated state. *J. Am. Chem. Soc.* 133, 18388–18396.
- (16) DeRose, V. J. (2003) Metal ion binding to catalytic RNA molecules. *Curr. Opin. Struct. Biol.* 13, 317–324.
- (17) Schnabl, J., and Sigel, R. K. (2010) Controlling ribozyme activity by metal ions. *Curr. Opin. Chem. Biol.* 14, 269–275.
- (18) Donghi, D., and Sigel, R. K. (2012) Metal ion-RNA interactions studied via multinuclear NMR. *Methods Mol. Biol.* 848, 253–273.
- (19) Johnson-Buck, A. E., McDowell, S. E., and Walter, N. G. (2011) Metal ions: Supporting actors in the playbook of small ribozymes. *Met. Ions Life Sci.* 9, 175–196.
- (20) Wedekind, J. E. (2011) Metal ion binding and function in natural and artificial small RNA enzymes from a structural perspective. *Met. Ions Life Sci.* 9, 299–345.
- (21) Murray, J. B., Seyhan, A. A., Walter, N. G., Burke, J. M., and Scott, W. G. (1998) The hammerhead, hairpin and VS ribozymes are catalytically proficient in monovalent cations alone. *Chem. Biol.* 5, 587–595.
- (22) Nakano, S., Chadalavada, D. M., and Bevilacqua, P. C. (2000) General acid-base catalysis in the mechanism of a hepatitis delta virus ribozyme. *Science* 287, 1493–1497.
- (23) Nakano, S., Proctor, D. J., and Bevilacqua, P. C. (2001) Mechanistic characterization of the HDV genomic ribozyme: Assessing the catalytic and structural contributions of divalent metal ions within a multichannel reaction mechanism. *Biochemistry* 40, 12022–12038.
- (24) Cerrone-Szkal, A. L., Siegfried, N. A., and Bevilacqua, P. C. (2008) Mechanistic characterization of the HDV genomic ribozyme: Solvent isotope effects and proton inventories in the absence of divalent metal ions support C75 as the general acid. *J. Am. Chem. Soc.* 130, 14504–14520.
- (25) O'Rear, J. L., Wang, S., Feig, A. L., Beigelman, L., Uhlenbeck, O. C., and Herschlag, D. (2001) Comparison of the hammerhead cleavage reactions stimulated by monovalent and divalent cations. *RNA* 7, 537–545.
- (26) Curtis, E. A., and Bartel, D. P. (2001) The hammerhead cleavage reaction in monovalent cations. *RNA* 7, 546–552.
- (27) Been, M. D. (2006) HDV ribozymes. *Curr. Top. Microbiol. Immunol.* 307, 47–65.
- (28) Nakano, S., Cerrone, A. L., and Bevilacqua, P. C. (2003) Mechanistic characterization of the HDV genomic ribozyme: Classifying the catalytic and structural metal ion sites within a multichannel reaction mechanism. *Biochemistry* 42, 2982–2994.
- (29) Chen, J. H., Yajima, R., Chadalavada, D. M., Chase, E., Bevilacqua, P. C., and Golden, B. L. (2010) A 1.9 Å crystal structure of the HDV ribozyme precleavage suggests both Lewis acid and general acid mechanisms contribute to phosphodiester cleavage. *Biochemistry* 49, 6508–6518.
- (30) Golden, B. L. (2011) Two distinct catalytic strategies in the hepatitis delta virus ribozyme cleavage reaction. *Biochemistry* 50, 9424–9433.
- (31) Fauzi, H., Kawakami, J., Nishikawa, F., and Nishikawa, S. (1997) Analysis of the cleavage reaction of a trans-acting human hepatitis delta virus ribozyme. *Nucleic Acids Res.* 25, 3124–3130.
- (32) Ferre-D'Amare, A. R., and Doudna, J. A. (2000) Crystallization and structure determination of a hepatitis delta virus ribozyme: Use of

the RNA-binding protein U1A as a crystallization module. *J. Mol. Biol.* 295, 541–556.

(33) Wadkins, T. S., Shih, I., Perrotta, A. T., and Been, M. D. (2001) A pH-sensitive RNA tertiary interaction affects self-cleavage activity of the HDV ribozymes in the absence of added divalent metal ion. *J. Mol. Biol.* 305, 1045–1055.

(34) Nakano, S., and Bevilacqua, P. C. (2007) Mechanistic characterization of the HDV genomic ribozyme: A mutant of the C41 motif provides insight into the positioning and thermodynamic linkage of metal ions and protons. *Biochemistry* 46, 3001–3012.

(35) Veeraraghavan, N., Bevilacqua, P. C., and Hammes-Schiffer, S. (2010) Long-distance communication in the HDV ribozyme: Insights from molecular dynamics and experiments. *J. Mol. Biol.* 402, 278–291.

(36) Wang, J., Cieplak, P., and Kollman, P. (2000) How well does a restrained electrostatic potential (RESP) model perform in calculating conformational energies of organic and biological macromolecules. *J. Comput. Chem.* 21, 1049–1074.

(37) Veeraraghavan, N., Ganguly, A., Chen, J. H., Bevilacqua, P. C., Hammes-Schiffer, S., and Golden, B. L. (2011) Metal binding motif in the active site of the HDV ribozyme binds divalent and monovalent ions. *Biochemistry* 50, 2672–2682.

(38) Jorgensen, W. L., Chandrasekhar, J., Madura, J. D., Impey, R., and Klein, M. L. (1983) Comparison of simple potential functions for simulating liquid water. *J. Chem. Phys.* 79, 926–935.

(39) Veeraraghavan, N., Ganguly, A., Golden, B. L., Bevilacqua, P. C., and Hammes-Schiffer, S. (2011) Mechanistic strategies in the HDV ribozyme: chelated and diffuse metal ion interactions and active site protonation. *J. Phys. Chem. B* 115, 8346–8357.

(40) Cornell, W. D., Cieplak, P., Bayly, C. I., Gould, I. R., Merz, K. M., Ferguson, D. M., Spellmeyer, D. C., Fox, T., Caldwell, J. W., and Kollman, P. A. (1995) A 2nd Generation Force-Field for the Simulation of Proteins, Nucleic-Acids, and Organic-Molecules. *J. Am. Chem. Soc.* 117, 5179–5197.

(41) Baker, N. A., Sept, D., Joseph, S., Holst, M. J., and McCammon, J. A. (2001) Electrostatics of nanosystems: Application to microtubules and the ribosome. *Proc. Natl. Acad. Sci. U.S.A.* 98, 10037–10041.

(42) Holst, M. (2001) Adaptive numerical treatment of elliptic systems on manifolds. *Advances in Computational Mathematics* 15, 139–191.

(43) Bank, R., and Holst, M. (2003) A new paradigm for parallel adaptive meshing algorithms. *SIAM Rev.* 45, 291–323.

(44) Chin, K., Sharp, K. A., Honig, B., and Pyle, A. M. (1999) Calculating the electrostatic properties of RNA provides new insights into molecular interactions and function. *Nat. Struct. Biol.* 6, 1055–1061.

(45) Misra, V. K., and Draper, D. E. (2000) Mg^{2+} binding to tRNA revisited: The nonlinear Poisson-Boltzmann model. *J. Mol. Biol.* 299, 813–825.

(46) Maderia, M., Hunsicker, L. M., and DeRose, V. J. (2000) Metal-phosphate interactions in the hammerhead ribozyme observed by ^{31}P NMR and phosphorothioate substitutions. *Biochemistry* 39, 12113–12120.

(47) Garcia-Garcia, C., and Draper, D. E. (2003) Electrostatic interactions in a peptide–RNA complex. *J. Mol. Biol.* 331, 75–88.

(48) Wang, T., Tomic, S., Gabdoulline, R. R., and Wade, R. C. (2004) How optimal are the binding energetics of barnase and barstar? *Biophys. J.* 87, 1618–1630.

(49) Misra, V. K., and Draper, D. E. (1998) On the role of magnesium ions in RNA stability. *Biopolymers* 48, 113–135.

(50) Hummer, G., Pratt, L. R., and Garcia, A. E. (1997) Ion sizes and finite-size corrections for ionic-solvation free energies. *J. Chem. Phys.* 107, 9275–9277.

(51) Misra, V. K., and Draper, D. E. (2001) A thermodynamic framework for Mg^{2+} binding to RNA. *Proc. Natl. Acad. Sci. U.S.A.* 98, 12456–12461.

(52) *The Pymol Molecular Graphics System*, version 1.5.0.4 (2012) Schrödinger, LLC, New York.

(53) Tanner, N. K., Schaff, S., Thill, G., Petit-Koskas, E., Crain-Denoyelle, A. M., and Westhof, E. (1994) A three-dimensional model of hepatitis delta virus ribozyme based on biochemical and mutational analyses. *Curr. Biol.* 4, 488–498.

(54) Perrotta, A. T., and Been, M. D. (1996) Core sequences and a cleavage site wobble pair required for HDV antigenomic ribozyme self-cleavage. *Nucleic Acids Res.* 24, 1314–1321.

(55) Leontis, N. B., Stombaugh, J., and Westhof, E. (2002) The non-Watson-Crick base pairs and their associated isostericity matrices. *Nucleic Acids Res.* 30, 3497–3531.

(56) Chen, J. H., Gong, B., Bevilacqua, P. C., Carey, P. R., and Golden, B. L. (2009) A catalytic metal ion interacts with the cleavage Site G·U wobble in the HDV ribozyme. *Biochemistry* 48, 1498–1507.

(57) Levesque, D., Raymond, C., and Perreault, J. P. (2012) Characterization of the trans Watson-Crick GU Bbase pair located in the catalytic core of the antigenomic HDV ribozyme. *PLoS One* 7, e40309.

(58) Izatt, R. M., Christensen, J. J., and Rytting, J. H. (1971) Sites and thermodynamic quantities associated with proton and metal ion interaction with ribonucleic acid, deoxyribonucleic acid, and their constituent bases, nucleosides, and nucleotides. *Chem. Rev.* 71, 439–481.

(59) Chadalavada, D. M., Knudsen, S. M., Nakano, S., and Bevilacqua, P. C. (2000) A role for upstream RNA structure in facilitating the catalytic fold of the genomic hepatitis delta virus ribozyme. *J. Mol. Biol.* 301, 349–367.

(60) Gresh, N., Sponer, J. E., Spackova, N., Leszczynski, J., and Sponer, J. (2003) Theoretical study of binding of hydrated $Zn(II)$ and $Mg(II)$ cations to 5'-guanosine monophosphate. Toward polarizable molecular mechanics for DNA and RNA. *J. Phys. Chem. B* 107, 8669–8681.

(61) Reblova, K., Spackova, N., Koca, J., Leontis, N. B., and Sponer, J. (2004) Long-residency hydration, cation binding, and dynamics of loop E/helix IV rRNA-L25 protein complex. *Biophys. J.* 87, 3397–3412.

(62) Cate, J. H., and Doudna, J. A. (1996) Metal-binding sites in the major groove of a large ribozyme domain. *Structure* 4, 1221–1229.

(63) Kieft, J. S., and Tinoco, I., Jr. (1997) Solution structure of a metal-binding site in the major groove of RNA complexed with cobalt(III) hexammine. *Structure* 5, 713–721.